

## Regular Articles

## Dynamic properties of a pulse-pumped fiber laser with a short, high-gain cavity

Chaolin Yang, Junhong Guo, Pu Wei, Hongdan Wan<sup>\*</sup>, Ji Xu, Jin Wang<sup>\*</sup>

Nanjing University of Posts and Telecommunications, Nanjing 210023, China

## ARTICLE INFO

## Article history:

Received 1 December 2015

Revised 30 April 2016

Accepted 29 May 2016

## Keywords:

Fiber laser

Pulse

Ring cavity

Adaptive-discrete-grid-finite-difference-method

## ABSTRACT

We demonstrate a pulsed high-gain all-fiber laser without intracavity modulators, where a short and heavily Erbium-doped fiber is used as the gain medium in a ring cavity. By pulsed-pumping this short high gain cavity and tuning an intracavity variable optical coupler, the laser generates optical pulses with a pulse-width of  $\mu\text{s}$  at a repetition rate in the order of kHz down to one-shot operation. Furthermore, dynamic properties of this laser are investigated theoretically based on a traveling-wave-model, in which an adaptive-discrete-grid-finite-difference-method is applied. The simulation results validate the experimental results. The demonstrated pulsed laser is compact, flexible and cost-effective, which will have great potential for applications in all-optical sensing and communication systems.

© 2016 Elsevier Inc. All rights reserved.

## 1. Introduction

Pulsed laser sources are very important instruments for scientific research and industrial applications, such as distributed fiber sensing and communication systems [1]. Among them, master-oscillator-power-amplifier (MOPA) and Q-switching laser are two commonly used methods. The MOPA features a great flexibility in the pulse duration and the repetition rate, but multi-stage amplifications are needed to realize high power output. The Q-switched fiber lasers can generate pulses with high peak power and high repetition rate [2]; however, most of them use intracavity modulators, which are costly and relatively bulky [3,4]. Recently, pulsed fiber lasers without intracavity modulators are proposed by seeding the linear cavity with pulse-modulated pump LDs [5–7]. Among most of them, linear cavity with long gain medium and free-space coupled multimode pump LDs are used. As a long gain medium may bring intensity noise, the use of free-space coupled optics could significantly complicate the package design, which becomes a challenging issue to maintain a stable laser output [8,9]. It still needs efforts to develop a pulsed fiber source with a simplified and stabilized structure as well as high tuning flexibility.

In this letter, we propose a simple and flexible pulsed fiber ring laser without any intracavity modulators, where a short and high-

gain medium, namely a heavily Er-doped fiber (HEDF), is used in the ring shaped cavity. By pulsed-pumping this cavity, the laser generates optical pulses with a pulse-width of  $\mu\text{s}$  at a repetition rate in the order of kHz down to one-shot operation. Laser pulses are tunable by modulating the pump power and adjusting a variable optical coupler (VOC). The tunability of the laser output is studied experimentally, while physical processes within this fiber laser are studied theoretically. To investigate the dynamic properties of the proposed laser, a numerical model based on adaptive-discrete-grid-finite-difference-method (ADGFDM) is developed.

## 2. Experimental setup

The schematic of the proposed laser is illustrated in Fig. 1. A WDM, a single-mode (SM) HEDF (LIEKKI Er110-4/125, nLIGHT), a fiber pigtailed ISO, an intracavity PC and a VOC are fiber-coupled which close-looped the ring cavity. The whole laser cavity is about 0.2 m long, where the HEDF has a length of about 0.1 m and is used as the gain fiber. The HEDF has a high doping level, low background loss ( $<0.02\text{ dB/m}$ ) and a high-gain per unit fiber length ( $\sim 1.1\text{ dB/cm}$ ). The pumping system consists of a 980 nm LD (driven by a pulsed electric driver) and is thermally stabilized by an ATC. The pump pulses coupled into the ring cavity have a peak power of about 500 mW. The pulse energy and width of the pump seeds can be set by varying the modulation voltage of the pulsed electric driver. Therefore, plus the adjustment of the VOC's intracavity coupling ratio  $r$  (from 0.1 to 0.9), the fiber laser output can be actively controlled. The laser spectra are measured by an optical spectrum

<sup>\*</sup> Corresponding authors.

E-mail addresses: [hdwan@njupt.edu.cn](mailto:hdwan@njupt.edu.cn) (H. Wan), [jinwang@njupt.edu.cn](mailto:jinwang@njupt.edu.cn) (J. Wang).

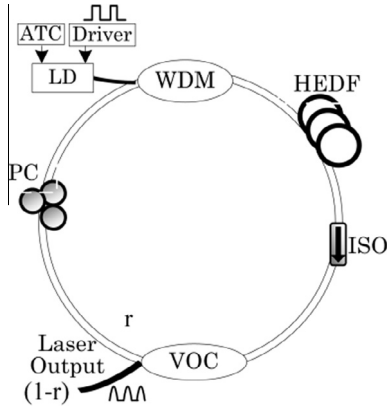


**Fig. 1.** Schematic of the proposed fiber laser. ATC: automatic temperature controller; WDM: wavelength division multiplexer; ISO: isolator; PC: polarization controller.

analyzer (86142B, Agilent). The laser energy per pulse and pulses' time shape are measured by a high speed photodetector and oscilloscope.

### 3. Experimental results and discussion

To illustrate the high-absorption performance and modulation of the considered ring cavity, the energy transfer property of the pulsed pumping scheme is first experimentally investigated. The optical spectra of the 980 nm pump LD were measured before and after a single pass of the HEDF. As shown in Fig. 2(a), the HEDF produces a 15 dB-absorption for the pump LD. The ASE spectrum of the amplified pulsed pump seed after the HEDF was also measured. As shown in Fig. 2(b), the ASE spectrum is peaked at 1561.6 nm with a bandwidth of 36.7 nm. It can also be seen in Fig. 2(a) that the pulsed-modulation induces spectral oscillations (rips) in the LD pump spectrum. However, due to the relatively longer lifetime of the  $\text{Er}^{3+}$ , the rips in the ASE spectrum is reduced via the amplification procedure, shown in the inset of Fig. 2(b).

After close-looping the ring cavity, the laser spectra were measured under different power and repetition rate of pump pulses. To build a laser oscillation for a set of coupling ratio  $r$ , there is a threshold value of the pump peak power  $P_{th}$  to achieve enough high intracavity gain and narrow band laser spectrum. As seen in Fig. 3, where the coupling ratio  $r$  is set to 0.9, the threshold  $P_{th}$  is about 100 mW. Also, with the same  $r$ , higher pump power generates higher oscillation amplitude. No excited-state absorption (ESA) was observed for different power powers during all the measurement time. Unlike other continuously pumped gain fibers, the pulsed-pump scheme eliminates the up-conversion and ion-

clustering effects. It should be noticed that for a pump peak power of 400 mW, the lasing output is indeed not stable. Thus, the dynamic process of this pulse-pumped fiber laser needs to be much more understood.

Fig. 4 shows the transient oscillation behavior of a single pulse under a pump peak power of 400 mW. The time for building up the population inversion and achieving a laser pulse is 2.5 ms. Since the pump power is not high enough as compared to the loss in the cavity, the laser power rises abruptly and undergoes a phase of spiking followed by relaxation subsequently. This type of oscillatory phenomenon in the pulse-pumped dynamics does not fall in the conventional picture of the CW pump regime: in the ring-shaped cavity, the pulsed pump power is re-absorbed in every intracavity circulation. However, as the cavity is short, the upper-state lifetime of  $\text{Er}^{3+}$  is longer than the cavity damping time and produce a relaxation oscillation, finally lead to a single-shot pulse as shown in Fig. 4.

By increasing the pump peak power to 500 mW, the laser oscillations finally settled to its steady-state oscillation. As shown in Fig. 5, Gauss shaped laser pulses with 8.71  $\mu\text{s}$  pulse duration are produced in the ring cavity, having a repetition rate of 4 kHz, which is in fact the same with the pump pulses. Experimental results show that: the higher pump energy used, the higher laser power and narrower pulse width are produced. Subject to the power limit of the pump SM LD, the highest peak power of laser pulses is 26 mW, when  $r$  is set to 0.9 and the pump pulses are peaked at 500 mW. Also, the pump efficiency rises with the increase of the repetition rate, because the population inversion decays less between the pulses at a higher repetition rate.

To further investigate the dynamic properties of this fiber laser theoretically, the traveling wave model in Ref. [10] is extended to satisfy this pulse pumped ring cavity. The spatial-temporal evolution of the system is given by the following PDEs:

$$\frac{\partial N_2}{\partial t} + \frac{N_2}{\tau} = \frac{\Gamma_p \lambda_p}{hcA} [\sigma_{ap} N_1 - \sigma_{ep} N_2] P_p + \frac{\Gamma_s \lambda_s}{hcA} [\sigma_{as} N_1 - \sigma_{es} N_2] P_s \quad (1)$$

$$\begin{aligned} \frac{P_{p(k)}^m - P_{p(k-e(p))}^m}{e(p)\Delta x} + \frac{1}{v_p} \frac{P_{p(k)}^{m+e(p)} - P_{p(k)}^m}{e(p)\Delta t} \\ = \Gamma_p [\sigma_{ep} N_2^m - \sigma_{ap} N_1^m] P_{p(k)}^m - \alpha_p P_{p(k)}^m \end{aligned} \quad (2)$$

$$\begin{aligned} \frac{P_{s(k)}^m - P_{s(k-e(p))}^m}{e(p)\Delta x} + \frac{1}{v_s} \frac{P_{s(k)}^{m+e(p)} - P_{s(k)}^m}{e(p)\Delta t} \\ = \Gamma_s [\sigma_{es} N_2^m - \sigma_{as} N_1^m] P_{s(k)}^m + \Gamma_s N_2^m \sigma_{es} 2hc^2 \Delta \lambda_s / \lambda_s^3 - \alpha_s P_{s(k)}^m \end{aligned} \quad (3)$$

$N_t$  is the  $\text{Er}^{3+}$  dopant concentration,  $N_1$  and  $N_2$  are the population densities of the ground and upper level, related by  $N_t = N_1 + N_2$ .  $\tau$  is the fluorescence lifetime, the pump and signal powers are represented by  $P_p$  and  $P_s$ , respectively,  $\lambda_{p(s)}$  is the pump (signal)

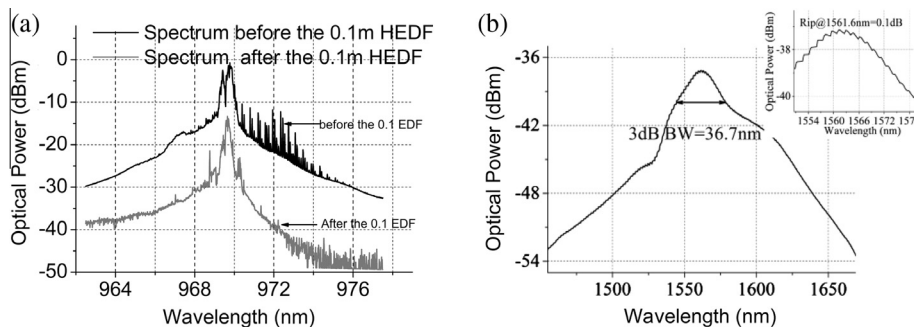


**Fig. 2.** (a) Optical spectra snapshots of the 980 nm pulsed pump LD with 200 mW peak power and 20  $\mu\text{s}$  pulse width; (b) ASE spectrum of the pulsed pump seed amplified by the 0.1 m HEDF.

Download English Version:

<https://daneshyari.com/en/article/464286>

Download Persian Version:

<https://daneshyari.com/article/464286>

[Daneshyari.com](https://daneshyari.com)